absence of a photodissociative pathway for energy dissipation in the molecular system.[7] In addition, the interpretation of the spectra would be greatly simplified by the presence of a single species in solution. This study addresses the vibrational population changes of deoxy-Hb as a result of absorption of a 436-nm and 532-nm photon by examining the anti-Stokes/Stokes intensity ratio of $\nu_7$, the strongest mode in the low-frequency region of the spectrum, as a function of laser fluence using 30-ps time resolution.

Representative transient resonance Raman spectra of both Stokes and anti-Stokes scattering in the 625–875-$cm^{-1}$ region of deoxy-Hb are shown in Figure 1. The picosecond Raman spectrometer used in this study has been described in detail elsewhere.[8] Three Raman-active heme modes, $\nu_7$, $\nu_{16}$, and $\nu_{32}$, at 671, 756, and 790 $cm^{-1}$, respectively, are observed in this spectral region. The anti-Stokes/Stokes intensity ratio of the totally symmetric heme mode, $\nu_7$, at 671 $cm^{-1}$ is found experimentally to be 8.6%. The spectra were fit with five Gaussian lines. The 841-$cm^{-1}$ propylene glycol line was used to correct for reabsorption effects of the respective scattering frequencies of the Stokes and anti-Stokes lines of $\nu_7$, following the formalism used by Schomaker and Champion.[9]

Three qualitative observations suggest that little or no heating occurs at the heme on the time scale of our experiments. First, the anti-Stokes/Stokes intensity ratios for all modes in the 625–875-$cm^{-1}$ region and the relative intensities of the anti-Stokes heme and solvent bands are independent of laser fluence. If the macrocycle were locally heated by absorption of an incident photon, the anti-Stokes/Stokes ratios of the heme modes would presumably display a power-dependent behavior distinctive from that of the solvent band. Second, spectra obtained with 10-ns pulses at an excitation wavelength identical with that of the 30-ps experiments yield an anti-Stokes/Stokes intensity ratio of 8.6% for the 674-$cm^{-1}$ heme mode. The heme is undoubtedly in thermal equilibrium with the bath on this time scale. Third, a two-pulse protocol using strong 532-nm pump pulses ($\sim 10^{10}$ W/$cm^2$) temporally and spatially overlapped with the 436-nm probe pulse also resulted in no change in the relative intensities of the anti-Stokes and Stokes heme modes. Collectively, these observations indicate that the macrocycle of deoxy-Hb is not "heated" within the 30-ps pulses.

In order to quantitatively extract vibrational populations (hence Boltzmann temperatures) from resonance scattering intensities, it is necessary to account for differences in resonance cross sections for Stokes and anti-Stokes processes. In the absence of B-term scattering,[10-12] the Kramers–Kronig transform technique provides a useful method of monitoring the population in the presence of complicating resonance effects. The inset in Figure 1 displays the relationship between the Boltzmann temperature and the observed anti-Stokes/Stokes intensity ratio of $\nu_7$ using a Kramers–Kronig transform technique and a first-order resonance Raman cross-section expression, which separates the thermal properties of the absorption line shape from the Bose–Einstein factor of the Raman mode. (For an excellent discussion of the applicability and limitations of the Kramers–Kronig transform technique on heme proteins, see ref 9, 12, and 13.) In the absence of resonance effects, the expected Boltzmann anti-Stokes/Stokes intensity ratio of $\nu_7$ at 300 K is 3.95%. After correction for reabsorption of the scattered light,[9] the transform technique predicts an anti-Stokes/Stokes intensity ratio of 8.2% for $\nu_7$ (see figure caption for details of analysis). On the basis of these studies, it is estimated that the average temperature during 30-ps pulses of the heme active site is 300 ± 30 K.

This study demonstrates that the excess energy resulting from the absorption of a visible photon does not produce Boltzmann heating at the active site of deoxy-Hb. This finding is totally consistent with the qualitative observations of the invariance of the intensity ratios of the anti-Stokes and Stokes lines to laser fluence. Finally, the observed ratios are quantitatively consistent with the ratios expected from application of the Kramers–Kronig transform technique. The simplistic concept of an equipartition of excess energy into vibrational modes of the heme appears to be invalid on this time scale. Further studies will probe the mode-specific relaxation processes ($T_1$ and $T_2$) of the heme using femtosecond and picosecond coherent and incoherent spectroscopies to elucidate the role vibrational dynamics plays in the short-time behavior of heme proteins.

(7) The Fe–CO dissociation energy has been found to be ~25 kcal/mol. (See: Keyes, M. H.; Falley, M.; Lumry, R. J. *J. Am. Chem. Soc.* **1971**, *93*, 2035.) In the studies of Petrich et al.,[2,3] substantial line-shape changes in $\nu_4$ occurred subsequent to photolysis using 580-nm excitation pulses (49 kcal/mol) and were attributed to a temperature rise of ~220 K. Their protocol supplied, at most, 24 kcal/mol of additional energy to the chromophore. The current study utilizes 436-nm excitation pulses, which deposit 66 kcal/mol of energy at the heme and thus would accentuate any heating effects.

(8) Courtney, S. H.; Jedju, T. M.; Friedman, J. M.; Alden, R. G.; Ondrias, M. R. *Chem. Phys. Lett.* **1989**, *164*, 39.

(9) Schomaker, K. T.; Champion, P. M. *J. Chem. Phys.* **1989**, *90*, 5982.

(10) Shelnutt, J. A.; Cheung, L. D.; Chang, R. C. C.; Yu, N.-T.; Felton, R. H. *J. Chem. Phys.* **1977**, *66*, 3387.

(11) Shelnutt, J. A. *J. Chem. Phys.* **1981**, *74*, 6644.

(12) Schomaker, K. T.; Champion, P. M. *J. Chem. Phys.* **1986**, *84*, 5314.

(13) Bangcharoenpaurpong, O.; Schomaker, K. T.; Champion, P. M. *J. Am. Chem. Soc.* **1984**, *106*, 5688.

## Metal-Assisted CO Insertion Reaction on a New Surface Rhodium Dimer Catalyst Observed by an in Situ Extended X-ray Absorption Fine Structure Technique

K. Asakura,† K. Kitamura-Bando,† K. Isobe,‡ H. Arakawa,§ and Y. Iwasawa*,†

*Department of Chemistry, Faculty of Science University of Tokyo, Hongo, Bunkyo-ku, Tokyo 113, Japan*
*Institute for Molecular Science 38 Saigo-naka, Myodaiji, Okazaki, Aichi 444, Japan*
*National Chemical Laboratory for Industry Tsukuba, Ibaraki 305, Japan*

*Received November 6, 1989*

The direct observation of structural changes of active sites at catalyst surfaces in a working state is a fascinating challenge.[1-4] Kitamura-Bando et al. prepared a new $SiO_2$-attached Rh-dimer catalyst active for $C_2H_4$ hydroformylation by the reaction between *trans*-$[Rh(C_5Me_5)(CH_3)]_2(\mu\text{-}CH_2)_2$ and surface OH groups of $SiO_2$.[5] They found that two CO per Rh dimer absorb to form twin-type carbonyls exhibiting IR bands at 2032–1969 $cm^{-1}$ and that the CO insertion into an alkyl group to form acyl proceeds by heating to 423–473 K under vacuum, while the reverse decarbonylation of the acyl group to form twin CO and alkyl occurs under ambient CO at room temperature. This behavior is opposite that observed with Rh-monomer catalysts in homogeneous systems. In the present article, we report the structure change of the $SiO_2$-attached Rh dimers during reversible CO insertion, which is a key step for hydroformylation, observed by an in situ EXAFS (extended X-ray absorption fine structure) technique.

$SiO_2$ (Aerosil 300, pretreated at 673 K for 1 h) was impregnated with a pentane solution of *trans*-$[Rh(C_5Me_5)(CH_3)]_2(\mu\text{-}CH_2)_2$[6] for 1 h at room temperature under high-purity Ar, followed by treatment at 313 K for 30 min and at 373 K for 1 h under vacuum to complete the surface reaction of the Rh complex with OH groups of $SiO_2$. The obtained $SiO_2$-attached Rh dimers were transferred to an in situ EXAFS cell without exposure to air.

† University of Tokyo.
‡ Institute for Molecular Science.
§ National Chemical Laboratory for Industry.

(1) Iwasawa, Y.; Asakura, K.; Ishii, H.; Kuroda, H. *Z. Phys. Chem.* **1985**, *144*, 105.
(2) Iwasawa, Y. *Adv. Catal.* **1987**, *35*, 187.
(3) Adakura, K.; Iwasawa, Y. *J. Phys. Chem.* **1989**, *93*, 4213.
(4) Asakura, K.; Iwasawa, Y. *Physica B* **1989**, *158*, 142.
(5) Kitamura-Bando, K.; Asakura, K.; Arakawa, H.; Sugi, Y.; Isobe, K.; Iwasawa, Y. *J. Chem. Soc., Chem. Commun.* in press.
(6) Isobe, K.; de Miguel, A. V.; Bailey, P. M.; Okeya, S.; Maitlis, P. M. *J. Chem. Soc., Dalton Trans* **1983**, 1411.

0002-7863/90/1512-3242$02.50/0 

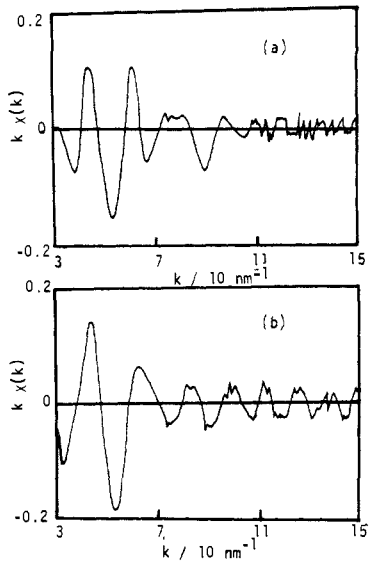


**Figure 1.** EXAFS oscillation for (a) species **2** and (b) species **3**.

EXAFS spectra were measured at BL-10B of the Photon Factory in a transmission mode. The EXAFS analysis was carried out by using the phase-shift and amplitude functions derived from Rh metal and $[Rh(CO)_2Cl]_2$.

The composition of the incipient attached Rh dimer (**1**) with the Rh–Rh distance of 0.262 nm was determined by gas-phase analysis, TPDE (temperature-programmed decomposition), and IR spectroscopy as shown in Scheme I.[5] After the exposure of species **1** to CO, the EXAFS oscillation above $k = 60$ nm$^{-1}$ disappeared, as shown in Figure 1a, indicating the cleavage of the Rh–Rh bonding. The cleavage of the Rh–Rh bonding was confirmed by the curve-fitting analysis of the inversely Fourier transformed data of the second Fourier peak in Figure 2a, which was due to Rh---O(carbonyl) bonding, as shown in Figure 2b. On heating of sample **2** at 423 K under vacuum, the twin CO bands disappeared and a new peak appeared at 1710 cm$^{-1}$ together with a small peak at 1394 cm$^{-1}$, indicating the formation of the acyl group as shown in Scheme I. The EXAFS oscillation above 60 nm$^{-1}$ reappeared by this treatment, as shown in Figure 1b.

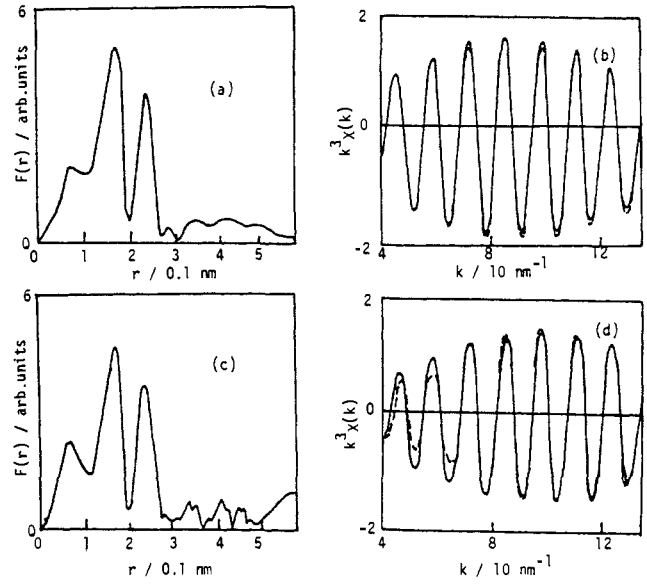


**Figure 2.** (a) EXAFS Fourier transform for species **2**, (b) curve-fitting analysis for the second peak of species **2**, (c) EXAFS Fourier transform for species **3**, and (d) curve-fitting analysis for the second peak of species **3**. Solid and broken lines in b and d show the observed data and the calculated curves based on Rh---O(carbonyl) (b) and Rh–Rh (d) models, respectively.

Curve-fitting analysis of the second shell peak in Figure 2c confirmed the existence of Rh–Rh at 0.270 nm as shown in Figure 2d, where the EXAFS envelope is different from that of Figure 2b because of the different back-scattering elements in the two cases. In this stage, the bridged carbene diminished, as proved by IR[5] analysis. When species **3** was exposed to CO at 313 K, the EXAFS oscillation disappeared, suggesting the cleavage of the Rh–Rh bond as shown in Scheme I. The formation and cleavage of the Rh–Rh bond in the $SiO_2$-attached Rh dimers were observed to be reversible by means of EXAFS.

In general, CO insertion reaction on mononuclear metal complexes proceeds favorably under high CO pressure and the decarbonylation of acyl groups takes place under vacuum. The CO insertion (ethyl migration) observed with the surface Rh dimers

**Scheme I.** Structure of the Attached Rh Dimers and Surface Structure Transformation during Reversible CO Insertion Reaction

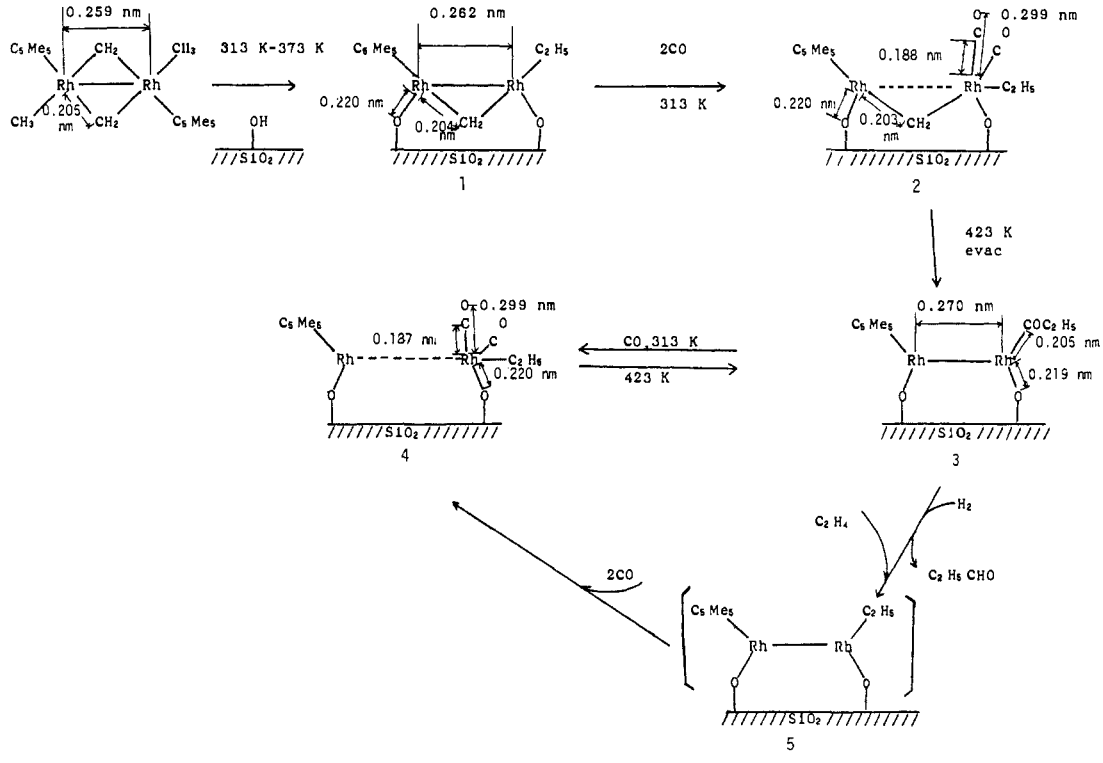

is converse and quite unique. It was found that the Rh-Rh bond was re-formed together with the formation of the acyl group. It is to be noted that species **2** and **4** with no Rh-Rh bonding do not act as monomers, but the CO insertion reaction was assisted by dimer formation. The vacant site on Rh produced by insertion of CO into the Rh-ethyl bond is replaced by the Rh-Rh metal bond to stabilize the acyl group. Similar metal-promoted CO insertions have been observed in homogeneous systems.[7,8] In these homogeneous systems, however, neither the reverse decarbonylation of acyl (COR) nor the reaction of the acyl group with $H_2$ to form aldehyde has been observed. The CO insertion mechanism has been discussed in the context of reaction steps for mononuclear metal complexes in homogeneous systems. However, the present work implies that CO insertion on the metal dimers and the surface of metal particles could proceed by the promotion of metal-metal bonding. The metal-assisted mechanism discussed here would be an example to explain the role of metal ensembles for metal catalysts.

(7) Collman, J. P.; Rothrock, R. K.; Finke, R. G.; Rose-Munch, F. *J. Am. Chem. Soc.* **1977**, *99*, 7381.
(8) Collman, J. P.; Rothrock, R. K.; Finke, R. G.; Mooew, E. J.; Rose-Munch, F. *Inorg. Chem.* **1982**, *21*, 146.

## Complexes Containing a $C_2$ Bridge between an Electron-Rich Metal and an Electron-Deficient Metal. An Agostic Interaction in a $RuCH_2CH_2Zr$ Moiety

R. Morris Bullock,* Frederick R. Lemke, and David J. Szalda†

*Department of Chemistry, Brookhaven National Laboratory Upton, New York 11973*

*Received November 20, 1989*

Complexes containing two metals of disparate electronic properties often exhibit unusual structural and reactivity features. Examples of such compounds include those in which early and late transition metals are joined by a direct metal-metal bond,[1] a bridging $CH_2$ ligand,[2] or a single carbon atom ($\mu_2$-carbide).[3] Complexes in which two metals are linked by a $C_2$ bridge have been far less extensively studied than the well-known bridging methylene[4] ($MCH_2M$) compounds. Dimetalloethanes ($MCH_2CH_2M$)[5] and dimetalloalkenes (MCH=CHM)[6] reported to date have either identical or similar electronic environments of the two metals. We report here the preparation of compounds which contain CH=CH and $CH_2CH_2$ bridges between an electron-rich $(C_5H_5)(PMe_3)_2Ru$ fragment and an electron-deficient $(C_5H_5)_2ZrCl$ moiety.

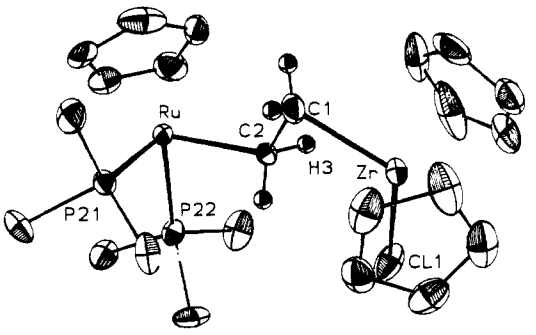


**Figure 1.** An ORTEP view of **3** (thermal ellipsoids at 50% probability level) with hydrogen atoms omitted except those on the bridging $CH_2CH_2$. The atoms Ru, C2, C1, Zr, and CL1 are approximately coplanar with the maximum deviation ±0.05 Å from the plane defined by these five atoms. The distance Zr-H3 is 2.19 (2) Å. Some other distances (Å) and angles (deg) are as follows: Zr-Cl, 2.276 (10); Zr-C2, 2.549 (9); Zr-CL1; 2.579 (3); Ru-C2, 2.186 (9); C1-C2, 1.485 (14); Zr-C1-C2, 82.5 (6); C1-C2-Ru, 118.2 (7); Cl-Zr-CL1; 117.4 (3); C2-H3-Zr, 100 (1).

Unsaturated carbon ligands bonded to late transition metals generally undergo $\beta$-attack by electrophiles and $\alpha$-attack by nucleophiles.[7] We have shown[8] that relatively acidic transition metal hydrides such as $(C_5H_5)(CO)_3MoH$ protonate the $\beta$-carbon of the metal alkynyl complex $(C_5H_5)(PMe_3)_2RuC{\equiv}CCH_3$ to give the ionic product $[(C_5H_5)(PMe_3)_2Ru{=}C{=}C(H)CH_3]^+$-$[(C_5H_5)(CO)_3Mo]^-$. Early transition metal hydrides typically exhibit hydridic rather than acidic reactivity.[9] Accordingly, the opposite regiochemistry is expected upon their reaction with ruthenium alkynyl complexes, with the H of the early-metal hydride being delivered to the $\alpha$-carbon of the alkynyl ligand. The reaction of $(C_5H_5)(PMe_3)_2RuC{\equiv}CH$[10] with $(C_5H_5)_2ZrHCl$ in toluene leads to formation of the dimetalloalkene complex $(C_5H_5)$-$(PMe_3)_2RuCH{=}CHZrCl(C_5H_5)_2$ (**1**) in 73-87% isolated yield[11] (Scheme I). Both of the vinyl protons of **1** appear as a doublet of triplets in the $^1H$ NMR spectrum, since they couple to each other ($J_{HH}$ = 18.7 Hz) as well as to the two equivalent phosphorus atoms. In $CD_2Cl_2$, the RuC*H* appears at $\delta$ 9.46 ($^3J_{PH}$ = 4.3 Hz) while the ZrC*H* resonance appears at $\delta$ 8.38 ($^4J_{PH}$ = 0.8 Hz). A particularly intriguing feature of the $^{13}C$ NMR spectrum was the value of $J_{CH}$ = 110 Hz observed for the carbon bonded to Ru ($\delta$ 114.7, $^2J_{PC}$ = 16 Hz in $CD_2Cl_2$). This low $J_{CH}$ value suggests an agostic[12] interaction between the CH and the unsaturated Zr center. A broad band at 2590 $cm^{-1}$ in the IR spectrum of **1** (which sharpened and shifted to 1900 $cm^{-1}$ in RuCD=CHZr) is assigned to the agostic $\nu_{CH}$. The NMR and IR data indicate that the agostic interaction is between Zr and the CH that is $\beta$ to Zr. Erker and co-workers have found[13] an agostic interaction in a closely

† Research collaborator at Brookhaven National Laboratory. Permanent address: Department of Natural Sciences, Baruch College, New York, NY 10010.

(1) (a) Casey, C. P.; Jordan, R. F.; Rheingold, A. L. *J. Am. Chem. Soc.* **1983**, *105*, 665-667; *Organometallics* **1984**, *3*, 504-506. (b) Casey, C. P.; Palermo, R. E.; Jordan, R. F.; Rheingold, A. L. *J. Am. Chem. Soc.* **1985**, *107*, 4597-4599. (c) Casey, C. P.; Palermo, R. E.; Rheingold, A. L. *J. Am. Chem. Soc.* **1986**, *108*, 549-550. (d) Casey, C. P.; Nagashima, H. *J. Am. Chem. Soc.* **1989**, *111*, 2352-2353. (e) Barger, P. T.; Bercaw, J. E. *J. Organomet. Chem.* **1980**, *201*, C39-C44; *Organometallics* **1984**, *3*, 278-284. (f) Sartain, W. J.; Selegue, J. P. *J. Am. Chem. Soc.* **1985**, *107*, 5818-5820; *Organometallics* **1987**, *6*, 1812-1815; *Organometallics* **1989**, *8*, 2153-2158. (g) Bruno, J. W.; Huffman, J. C.; Green, M. A.; Caulton, K. G. *J. Am. Chem. Soc.* **1984**, *106*, 8310-8312.

(2) (a) Ozawa, F.; Park, J. W.; Mackenzie, P. B.; Schaefer, W. P.; Henling, L. M.; Grubbs, R. H. *J. Am. Chem. Soc.* **1989**, *111*, 1319-1327. (b) Mackenzie, P. B.; Coots, R. J.; Grubbs, R. H. *Organometallics* **1989**, *8*, 8-14. (c) Park, J. W.; Mackenzie, P. B.; Schaefer, W. P.; Grubbs, R. H. *J. Am. Chem. Soc.* **1986**, *108*, 6402-6404. (d) Mackenzie, P. B.; Ott, K. C.; Grubbs, R. H. *Pure Appl. Chem.* **1984**, *56*, 59-61. (e) Jacobsen, E. N.; Goldberg, K. I.; Bergman, R. G. *J. Am. Chem. Soc.* **1988**, *110*, 3706-3707. (f) Goldberg, K. I.; Bergman, R. G. *J. Am. Chem. Soc.* **1988**, *110*, 4853-4855.

(3) Latesky, S. L.; Selegue, J. P. *J. Am. Chem. Soc.* **1987**, *109*, 4731-4733.

(4) Herrmann, W. A. *Adv. Organomet. Chem.* **1982**, *20*, 159-263.

(5) Beck and co-workers have developed a method for the synthesis of hydrocarbon-bridged bimetallic compounds by reaction of metal anions with cationic metal complexes containing $\pi$-bonded hydrocarbons. For a review of this work, see: Beck, W. *Polyhedron* **1988**, *7*, 2255-2261.

(6) For leading references to dimetalloalkenes, see: (a) Hoffman, D. M.; Hoffmann, R. *Organometallics* **1982**, *1*, 1299-1302. (b) Targos, T. S.; Geoffroy, G. L.; Rheingold, A. L. *Organometallics* **1986**, *5*, 12-16. (c) Mague, J. T. *Organometallics* **1986**, *5*, 918-926.

(7) (a) Davison, A.; Selegue, J. P. *J. Am. Chem. Soc.* **1978**, *100*, 7763-7765; **1980**, *102*, 2455-2456. (b) Bruce, M. I.; Swincer, A. G. *Adv. Organomet. Chem.* **1983**, *22*, 59-128 and references cited therein.

(8) Bullock, R. M. *J. Am. Chem. Soc.* **1987**, *109*, 8087-8089.

(9) (a) Labinger, J. A.; Komadina, K. H. *J. Organomet. Chem.* **1978**, *155*, C25-C28. (b) Wolczanski, P. T.; Bercaw, J. E. *Acc. Chem. Res.* **1980**, *13*, 121-127. (c) Schwartz, J.; Labinger, J. A. *Angew. Chem., Int. Ed. Engl.* **1976**, *15*, 333-340.

(10) Bullock, R. M. *J. Chem. Soc., Chem. Commun.* **1989**, 165-167.

(11) Complete spectroscopic data for **1**, **1**-$d_1$, **2**, **3**, and **3**-$d_1$ are provided in the supplementary material.

(12) Brookhart, M.; Green, M. L. H.; Wong, L.-L. *Prog. Inorg. Chem.* **1988**, *36*, 1-124.

(13) Erker, G.; Frömberg, W.; Angermund, K.; Schlund, R.; Krüger, C. *J. Chem. Soc., Chem. Commun.* **1986**, 372-374.

0002-7863/90/1512-3244$02.50/0 